SYMMETRY-BASED DETECTION OF NUCLEI IN MICROSCOPY IMAGES

Sundaresh Ram and Jeffrey J. Rodríguez

Department of Electrical and Computer Engineering
University of Arizona, Tucson, AZ 85721, USA
{ram1,jrod}@ece.arizona.edu

ABSTRACT

Accurate detection of individual cell nuclei in microscopic images is an essential task for many biological studies. Blur, clutter, bleed through, imaging noise and touching and partially overlapping nuclei with varying sizes and shapes make automated detection of individual cell nuclei a challenging task using image analysis. In this paper we propose an automated method for robust detection of individual cell nuclei in fluorescence *in-situ* hybridization (FISH) images obtained via confocal microscopy. Our algorithm consists of the following steps: image denoising, binarization, detection of nuclear seed points combining the fast radial symmetric transform (FRST) and a distance-based non-maximum suppression. We show that our algorithm provides improved detection accuracy compared to the existing algorithms.

***Index Terms*—** Nucleus detection, FRST, FISH images, unimodal thresholding.

1. INTRODUCTION

The detection of cells in fluorescent *in-situ* hybridization (FISH) images is an important first task for many biological studies including high throughput analysis of gene expression level, morphology, and quantifying molecular markers and phenotypes in a single cell. Counting cells or knowing the concentration of specific cells such as red blood cells, viruses and pathogens in medicine can reveal important information about the progress of an infectious disease. Studies that examine the growth rate of microorganisms also require cell counting. Also cell migrations and deformations play an essential role in biological processes, such as parasite invasion, immune response, embryonic development, and cancer detection. Thus, there is a significant interest in these applications to be able to detect the cell nuclei with high accuracy.

Manual cell counting by visual inspection is difficult, labor intensive, time consuming, and a fatiguing process. This is due to various reasons such as fluctuating intensities and morphological variations of the cells within images [1], variances in illumination [2], crowding and overlapping of cells of varying sizes and shapes, accidental and non-specific staining, low signal-to-ratio (SNR) [3], spectral unmixing errors, microscopy imaging limitations and the large number of cells that the pathologist has to count per image. Moreover, the estimated cell counts using manual analysis are not reproducible, as the task can be subjective, differing from person to person, and even one time to another. These factors serve as a motivation for designing an automated algorithm for the detection of cell nuclei. However, for the reasons mentioned above, the design of such an algorithm is challenging.

The commonly available software for cell detection is usually based on traditional and classical techniques such as correlation matching, global thresholding, morphological operations and energy minimization and optimization. These techniques suffer considerably due to over-generalization, limiting their use on images gathered in cell biology research. To overcome their inherent limitations, existing software tools often have user interfaces that allow users to manually edit the results obtained. This, however, negates the benefits of automation such as speed and reproducibility. Recently, several new methods have been proposed for automated nucleus detection [2–12]. Al-Kofahi *et al*. [3] proposed a cell detection algorithm using a multiscale Laplacian-of-Gaussian (LoG) filtering constrained by distance-map-based adaptive scale selection. This method suffers from two drawbacks: 1) it requires a bimodal histogram, and 2) for large and highly textured cells, it often finds multiple seeds within one nucleus. Parvin *et al*. [7] introduced the iterative voting method, which uses oriented kernels for inferring saliency of objects in order to detect them. This method produces false seeds in the overlapping cell regions, when the intensity of the overlapping cell regions is brighter (or darker) than the non-overlapping regions within individual cells. Qi *et al*. [8] reported a cell detection algorithm that utilizes single-path voting followed by mean-shift clustering. This method performs well when we have a uniform cell size within an image, but detects false seeds when the cells are varying in size and shape.

In this paper we propose an automated technique to detect the cell nuclei of *Drosophila melanogaster* obtained via confocal microscopy. We reduce noise using the multiscale variance stabilizing transform (MS-VST), binarize the images using a histogram thresholding technique, create a response image using the fast radial symmetric transform (FRST), and finally obtain a single seed/marker for every nucleus using distance-based non-maximum suppression.

2. METHODS

The ovarian germ-line of the *Drosophila melanogaster* consists of two types of cells, namely “nurse cells" and “follicle cells". The follicle cells are smaller than the nurse cells and surround the nurse cells in an elliptical fashion. Fig.1a shows a single slice of a 3-D data set with nurse cells surrounded by follicle cells.

2.1. Image denoising

We use Zhang’s denoising method (MS-VST) [13], which is particularly suited for confocal microscope images, to suppress the background noise of the images, thereby increasing the contrast between the foreground nuclei and the surrounding background. The MS-VST models the image as a mixed Poisson-Gaussian (MPG) process. Thus, an observed image I_n is given by

$$I_n = \alpha X_n + Y_n,\ X_n \sim \mathcal{P}(\lambda_n),\ Y_n \sim \mathcal{N}(\mu_n, \sigma_n^2) \qquad (1)$$

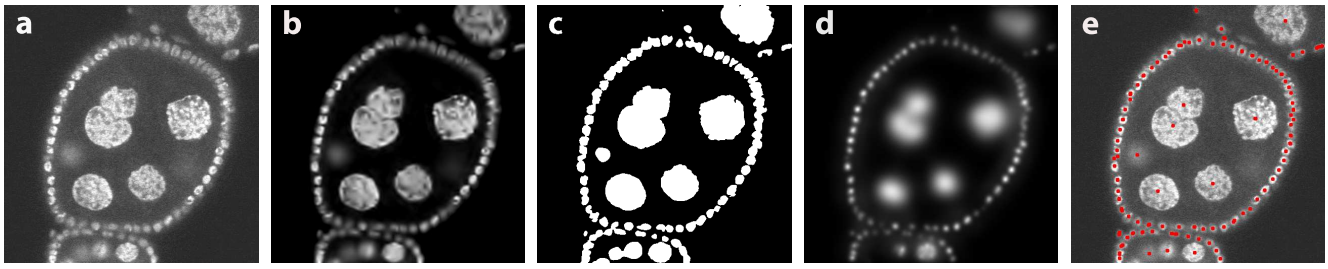

Fig. 1: (a) Original image. (b) Denoised image. (c) Image after thresholding and additional refinements. (d) Image after applying FRST. (e) Detected seeds superimposed (red) onto original image after non-maximum suppression.

where $\alpha > 0$ is the overall gain of the detector, X_n is the Poisson variable modeling the photon counting, Y_n is a normal variable representing readout noise and X_n and Y_n are assumed mutually independent. The goal here is to use a MS-VST to Gaussianize the filtered MPG process using the isotropic undecimated wavelet transform as a filter and detect the significant filter coefficients in order to suppress the noise. The unknown parameters α, μ, and σ are estimated from samples in a uniform region within the image background. An example image after denoising is shown in Fig. 1b.

2.2. Thresholding

The MS-VST denoising enhances the separation between modes in the bimodal histogram of each image. For our image data, the foreground nuclei regions correspond to the peak in the histogram at the large gray levels. We employ Otsu's thresholding [14] to remove the peak in the histogram corresponding to small gray level values. The residual histogram is unimodal with a steep monotonic increase till a peak is reached, followed by a Gaussian-like decay that corresponds to the foreground nuclei regions. We use Rosin's method [15] to find a threshold and identify the foreground nucleus regions. Due to the textures and intensity fluctuations present within the nuclei, some parts of the nuclei get detected as background.We make two refinements: 1) fill all the holes within each nucleus, where a hole is defined as a set of pixels that cannot be reached by filling in the background from the edge of the image and 2) dilate each region using a disk structuring element with a two-pixel radius. Fig. 1c shows the result after thresholding and the additional refinements.

2.3. Fast radial symmetric transform

Thresholding the denoised images finds foreground nuclei, which appear combined together in areas where they are densely populated. Thresholding helps to detect the individual foreground nuclei in areas where they are sparsely populated, but in areas where the nuclei appear clustered we still need to detect the individual nuclei. For this purpose we use the FRST method proposed by Loy *et al*. [16]. The FRST is a computationally efficient, non-iterative procedure that computes the centers of radial symmetry along varying radii $\rho_{\min} \leq \rho \leq \rho_{\max}$ by operating along the direction of the image gradient. Since nuclei are somewhat radially symmetric objects, this operation is well suited for their localization. To produce the candidate nuclei locations, first the gradient $g(x)$ is calculated at each pixel x. For each integer radius ρ, an *orientation projection image* O_ρ and a *magnitude projection image* M_ρ are formed. These images are generated by examining the gradient g at a point x, from which a *positively affected pixel* $P_+(x)$ and a *negatively affected pixel* $P_-(x)$ are determined. The *positively affected pixel* is that pixel which the gradient $g(x)$ is pointing to, at a distance ρ from the location x, and the *negatively affected pixel* is that pixel which the gradient $g(x)$ is pointing away from, at a distance ρ from the location x. The coordinates of $P_+(x)$ and $P_-(x)$ are given by the following equations.

$$P_+(x) = x + round\left(\frac{g(x)}{\parallel g(x) \parallel}\rho\right) \tag{2}$$

$$P_-(x) = x - round\left(\frac{g(x)}{\parallel g(x) \parallel}\rho\right) \tag{3}$$

The orientation and magnitude projection images are initially zero. For each pair $(P_+(x), P_-(x))$ of affected pixels, the corresponding pixel $P_+(x)$ in the image O_n and in the image M_n is incremented by 1 and $\parallel g(x) \parallel$, respectively, while the corresponding pixel $P_-(x)$ is decremented by the same quantities. The radial symmetry contribution at radius ρ is defined as a convolution

$$S_\rho = F_\rho * G_\rho, \tag{4}$$

where

$$\begin{aligned} F_\rho(x) &= \frac{M_\rho(x)}{k_\rho}\left(\frac{\mid \tilde{O}_\rho(x) \mid}{k_\rho}\right)^\gamma \\ \tilde{O}_\rho(x) &= \begin{cases} O_\rho(x) & \text{if } \mid O_\rho(x) \mid < k_\rho \\ k_\rho & \text{otherwise} \end{cases} \end{aligned} \tag{5}$$

G_ρ is a two dimensional Gaussian, γ is the radial strictness parameter, and k_ρ is a scaling factor that normalizes M_ρ and O_ρ across different radii.

The FRST transform is defined as the average of the symmetry contributions over all radii considered,

$$S = \frac{1}{\mid N \mid}\sum_{\rho \in N} S_\rho \tag{6}$$

where N is the set of radii being considered. In order to increase the computational speed of the algorithm, we compute the transform only at the *positively affected pixels* $P_+(x)$ and ignore the computation at *negatively affected pixels* $P_-(x)$ when we determine O_ρ and M_ρ, as our interest lies in the foreground nuclei regions, which appear brighter than the background. Also, we use a fixed G_ρ for all the radii. We apply this transform to the original image masked by the binarization obtained from Section 2.2. This yields an output response image. Fig. 1d shows the resultant response image generated after applying the FRST.

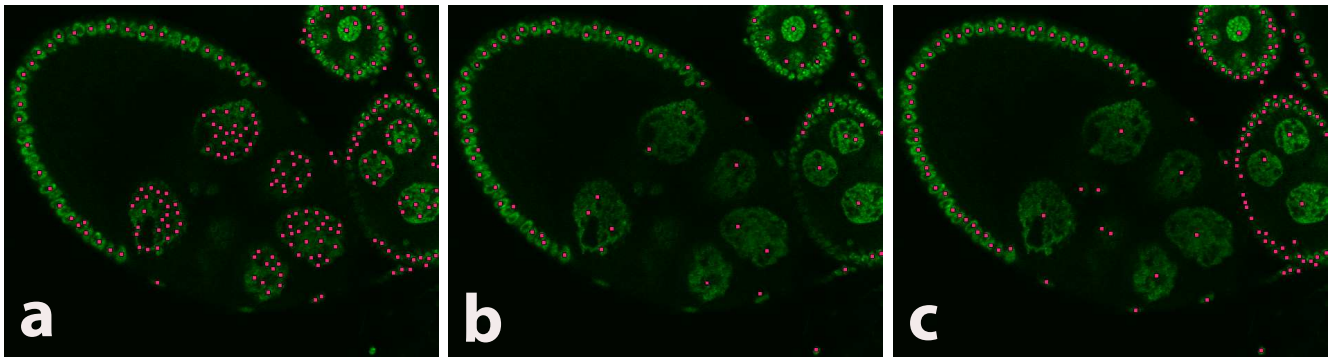

Fig. 2: Detections results on an image from the data set using: (a) Kofahi's MS-LoG method, (b) Parvin's IRV-K method and (c) our method.

2.4. Distance-based non-maximum suppression

Since our image data consists of highly textured cell nuclei, the response image generated by carrying out the FRST transform may sometimes contain multiple small peaks located very close to the true large peak (to be detected) within the nurse cells (large cells) . Also, in the densely populated regions where the nuclei appear clustered, the generated response image may at times contain erroneous small peaks in addition to the true peaks of the clustered nuclei, roughly equidistant from each of them. In order to overcome the two difficulties presented above and to obtain exactly one seed/marker per nucleus, we perform the following procedure: 1) grayscale dilation on the response image using a flat structuring element of size δ and 2) non-maximum suppression of the dilated image.

The grayscale dilation of $A(x, y)$ by a flat structuring element $B(x, y)$ that has zero height everywhere is defined as

$$(A \oplus B)(x, y) = \max\left\{A(x - x', y - y')|(x', y') \in D_B\right\} \quad (7)$$

where D_B is the domain of the structuring element B and $A(x, y)$ is assumed to be $-\infty$ outside the domain of the image. From (7) we can say that a grayscale dilation using a flat structuring element is a local-maximum operator. Thus, performing such a grayscale dilation with a structuring element of size δ gets rid of the small and erroneous peaks present within the response image. We then apply the non-maximum suppression on the dilated image. Following such a procedure, we usually obtain exactly one seed per nucleus. Fig. 1e shows the detected seeds using the grayscale dilation and non-maximum suppression overlaid (red) on the original image.

3. EXPERIMENTS AND RESULTS

The images were acquired using the Zeiss LSM 510 Meta confocal microscope. The x- and y-dimensions of each image acquired is 504×512 pixels, with a sampling interval of 0.31μm in both dimensions. We collected an image data set of 157 images consisting a total of 1386 cells (41 nurse cells and 1345 follicle cells). A careful manual segmentation of all the 157 images was performed and these segmentations were considered as the ground truth for all subsequent analysis. We compared our cell nuclei detection algorithm with Al-Kofahi's multiscale Laplacian-of-Gaussian (MS-LoG) cell detection algorithm [3] and Parvin's iterative radial voting scheme using oriented kernels (IRV-K) [7].

3.1. Algorithm parameter settings

For each image in our data set, in the denoising step the values of the unknown parameters α, μ, and σ are found by selecting a uniform region within the image background. To find a uniform region within the image background, we consider pixels belonging to the top quartile of the lowpass-filtered histogram of the original image. The remaining unknown parameters of our proposed algorithm are chosen and fixed for all the images in our data set as follows. In the FRST transform the radius is varied over the range

$$1 \leq \rho \leq 2 \times \max\{D(x, y)\} \quad (8)$$

where $D(x, y)$ is the distance transform of the binarized image. The variance of the Gaussian kernel is $\sigma_\rho^2 = \frac{1}{2}\rho$ for each $\rho \in [\rho_{\min}, \rho_{\max}]$. The optimal values for the radial strictness parameter and scaling factor in FRST and the structuring element size δ for grayscale dilation were selected using the receiver operating characteristic (ROC) curves by varying one parameter at a time while keeping the others fixed and choosing that value of the parameter which maximized the area under the curve (AUC). The radial strictness parameter is $\gamma = 2$, and the scaling factor $k_\rho = 10$. For the grayscale dilation, the structuring element size is $\delta = 11$.

3.2. Performance evaluation

The MS-LoG, IRV-K, and our proposed algorithm were run on our image data set to detect the nurse and follicle cells. We evaluated these algorithms using two conventional metrics that have been used for the evaluation of automated cell detection algorithms, namely coverage measure (F_β-Score) [6], [9], and pixelwise distance error E [8].

3.2.1. Coverage measure

The performance metric for comparing the detection accuracy of all the automated algorithms is obtained using the F_β-Score, also known as the coverage measure, defined by

$$F_\beta = (1 + \beta^2) \cdot \frac{\mathcal{P} \cdot \mathcal{R}}{(\beta^2 \cdot \mathcal{P}) + \mathcal{R}} \quad (9)$$

where $\mathcal{P}$ is precision and $\mathcal{R}$ is recall, defined by

$$\mathcal{P} = \frac{TP}{TP + FP}, \quad \mathcal{R} = \frac{TP}{TP + FN}$$

Table 1: PERFORMANCE OF THE DETECTION ALGORITHMS

Methods	F-Score	Distance Error E	
		mean	s.d.
Our Method	0.825	7.016	1.543
MS-LoG	0.718	8.261	1.639
IRV-K	0.764	7.835	2.048

where TP is the number of true positive detections, FP is the number of false positive detections and FN is the number of false negative detections. In this paper we use F_1(i.e., $\beta = 1$) as this is the most common choice for this type of evaluation.

3.2.2. Pixelwise distance error

The pixelwise distance error E is the mean pixelwise Euclidean distance between the centroids of the manually segmented nuclei and the the corresponding seed locations that were extracted using the automated segmentation algorithms, averaged over all nuclei and all images.

3.3. Results

The goal is to maximize the F_β-score and minimize the pixelwise distance error E. We present in Table 1 the comparison of these two metrics for the three automated algorithms, computed over all of our data set. Table 1 shows that our algorithm has the highest F_β-score and the lowest pixelwise distance error E, which indicates that it is the most accurate of these cell detectors. Fig. 2 shows the detection results on one image from our data set comparing the three detection algorithms. Fig. 2 shows that our method is usually able to detect exactly one seed/marker per nucleus. Also, in areas where the SNR is low (lower middle region and the lower right corner of the image), our algorithm is able to detect the cell nuclei with more accuracy when compared to the other two methods.

4. CONCLUSIONS

Accurate detection of individual cell nuclei in microscopy images is a challenging task for a manual user, as well as for any automated cell detection algorithm. Our method combines the MS-VST filtering to suppress the noise, histogram based thresholding to find the foreground regions and computation of the FRST and a distance-based non-maximum suppression to find and detect the individual cell nuclei. Parvin *et al*. [7] use an iterative radial voting scheme and Qi *et al*. [8] use a single-pass voting followed by a mean-shift clustering to detect the cells. Both these methods assume an estimated average diameter for the cells and uses a fixed value of radial range. Al-Kofahi *et al*. [3] takes a different approach by using a multiscale LoG filtering constrained by an adaptive scale selection in order to detect the cells. Our approach differs from these earlier methods. We do not choose a fixed radial range or do an adaptive scale selection as the key idea of the work presented in this paper is to be able to detect cells with varying sizes and high texture or fluctuating intensities within them, which was not considered in these earlier studies. The results demonstrate the improved performance of our algorithm, according to both the performance metrics considered.

5. ACKNOWLEDGMENTS

We thank Prof. Giovanni Bosco (Dept. of Genetics, Dartmouth College) for providing the confocal microscopy images used in this study.

6. REFERENCES

[1] S. Ram, J.J. Rodríguez, and G. Bosco, "Size-invariant cell nucleus segmentation in 3-d microscopy," in *Proc. IEEE Southwest Symp. Image Analysis and Interpretation*, 2012, pp. 37–40.

[2] M.E. Plissiti, C. Nikou, and A. Charchanti, "Automated detection of cell nuclei in pap smear image using morphological reconstruction and clustering," *IEEE Trans. Inf. Technol. Biomed.*, vol. 15, no. 2, pp. 233–241, Mar. 2011.

[3] Y. Al-Kofahi, W. Lassoued, W. Lee, and B. Roysam, "Improved automatic detection and segmentation of cell nuclei in histopathology images," *IEEE Trans. Biomed. Eng.*, vol. 57, no. 4, pp. 841–852, Apr. 2010.

[4] J.D. Vylder, J. Aelterman, M. Vandewoestyne, T. Lepez, D. Deforce, and W. Philips, "Cell nuclei detection using globally optimal active contours with shape prior," in *Advances in Visual Computing*. Springer Verlag, 2012, vol. 7432, pp. 115–124.

[5] C. Jung and C. Kim, "Segmenting clustered nuclei using h-minima transform-based marker extraction and contour parameterization," *IEEE Trans. Biomed. Eng.*, vol. 57, no. 10, pp. 2600–2604, Oct. 2010.

[6] P. Yan, X. Zhou, M. Shah, and S.T.C. Wong, "Automatic segmentation of high-throughput rnai fluorescent cellular images," *IEEE Trans. Inf. Technol. Biomed.*, vol. 12, no. 1, pp. 109–117, Jan. 2008.

[7] B. Parvin, Q. Yang, J. Han, H. Chang, B. Rydberg, and M.H. Barcellos-Hoff, "Iterative voting for inference of structural saliency and characterization of subcellular events," *IEEE Trans. Image Process.*, vol. 16, no. 3, pp. 615–623, Mar. 2007.

[8] X. Qi, F. Xing, D.J. Foran, and L. Yang, "Robust segmentation of overlapping cells in histopathology specimens using parallel seed detection and repulsive level set," *IEEE Trans. Biomed. Eng.*, vol. 59, no. 3, pp. 754–765, Mar. 2012.

[9] P. Quelhas, M. Marcuzzo, A.M. Mendonca, and A. Campilho, "Cell nuclei and cytoplasm joint segmentation using the sliding band filter," *IEEE Trans. Med. Imag.*, vol. 29, no. 8, pp. 1463–1473, Aug. 2010.

[10] Q. Wen, H. Chang, and B. Parvin, "A delaunay triangulation approach for segmenting clumps of nuclei," in *Proc. IEEE Int. Symp. Biomedical Imaging*, 2009, pp. 9–12.

[11] W. Xiong, S.C. Chia, and J.H. Lim, "Automated nuclei clump decomposition for image analysis in neuronal cell fluorescent microscopy," in *Proc. IEEE Int. Conf. Image Processing*, 2011, pp. 1577–1580.

[12] K.N. Chaudhury, Zs. Püspöki, A. Muñoz-Barrutia, D. Sage, and M. Unser, "Fast detection of cells using a continuously scalable mexican-hat-like template," in *Proc. IEEE Int. Symp. Biomedical Imaging*, 2010, pp. 1277–1280.

[13] B. Zhang, M.J. Fadili, J.-L. Starck, and J.-C. Olivo-Marin, "Multiscale variance-stabilizing transform for mixed-poisson-gaussian processes and its applications in bioimaging," in *Proc. IEEE Int. Conf. Image Processing*, 2007, pp. 233–236.

[14] N. Otsu, "A threshold selection method from gray-level histograms," *IEEE Trans. syst. Man Cybern.*, vol. SMC-9, no. 1, pp. 62–66, Jan. 1979.

[15] P. Rosin, "Unimodal thresholding," *Pattern Recognition*, vol. 34, no. 11, pp. 2083–2096, Nov. 2001.

[16] G. Loy and A. Zelinsky, "Fast radial symmetry for detecting points of interest," *IEEE Trans. Pattern Anal. Mach. Intell.*, vol. 25, no. 8, pp. 959–973, Aug. 2003.